Soft Matter

Cite this: *Soft Matter*, 2012, **8**, 7258

www.rsc.org/softmatter

PAPER

Micro-DSC, rheological and NMR investigations of the gelation of gallic acid and xyloglucan

Namon Hirun,[a] Hongqian Bao,[b] Lin Li,[b] G. Roshan Deen[c] and Vimon Tantishaiyakul*[a]

Received 9th January 2012, Accepted 30th April 2012
DOI: 10.1039/c2sm25056j

A novel thermoreversible gelling system consisting of tamarind seed xyloglucan (TSX) and gallic acid (GA) was prepared and investigated. The thermal transition temperatures obtained from both micro-DSC and viscoelastic methods were consistent. The hysteresis was observed for the GA–TSX gelling system. The hydrogen bonding interactions between GA and TSX were detected using ^{13}C nuclear magnetic resonance analyses. The carboxylic acid and the hydroxyl group at the *para* position of GA are the principal groups that interact with TSX. A low temperature induced intermolecular aggregation of TSX *via* hydrogen bonds between GA and TSX, leading to the formation of a gel network. The thermal stability of the GA–TSX gel increased with increasing the GA concentration. The viscoelastic behavior of the GA–TSX mixtures depended on the concentration of GA. For the mixture of GA and 1% (w/v) TSX, the critical gel concentration of GA was 0.69% (w/v) at physiological temperature (37 °C) and the sol–gel transition was well described by the scaling law. Moreover, the dried GA–TSX gels exhibited various morphologies that reflected the dependence of the arrangement of the TSX chains on the GA concentration.

Introduction

A thermoreversible gel can change from a liquid (solution, sol) to a solid (gel), and *vice versa*, in response to a change in environmental temperature. This type of gel has been comprehensively investigated as an intelligent material for biomedical applications.[1] Thermoreversible materials that exhibit the sol–gel transition may be natural or synthetic. However, most of these materials lack a proper viscoelastic behavior at a physiological temperature which is required for a medical application. Therefore, cross-linking strategies have been employed to produce the desired viscoelastic properties.[2] Generally, there are two types of cross-linking: chemical and physical. Chemical cross-linking involves the formation of covalent bonds, while physical cross-linking relies on non-covalent bonds or interactions such as ionic interaction, hydrophobic interaction, van der Waals forces or hydrogen bonds.[3] Chemically cross-linked gels lack a reversible property.[4] Gels that are physically cross-linked can be thermoreversible and therefore have been more widely developed for use as biomedical materials.

Xyloglucan is a polysaccharide extracted from higher plant cell walls. A major source of commercial xyloglucan comes from the seeds of *Tamarindus indica* which is grown extensively in Southeast Asia.[5] Tamarind seed xyloglucan (TSX) is composed of a cellulose main chain that is partially substituted with xylose or galacto-xylose side chains. Currently, this polymer has been explored for biomedical applications due to its biodegradability, biocompatibility, bioadhesivity and nontoxicity.[6–8] Generally, native or unmodified TSX cannot form a gel but it can exhibit a gelation behavior when some galactose residues are removed[9] or when it is mixed with some small molecules such as Eriochrome Black T,[10] alcohols,[11] epigallocatechin gallate, iodine[12] and congo red.[13]

Gallic acid (GA), 3,4,5-trihydroxybenzoic acid, has attracted much attention because it exhibits significant biological activities such as antioxidant, cardioprotective, antihyperglycaemic, antimutagenic and anticarcinogenic activities.[14–16] GA can form a gel with melamine.[17] However, gelation of a biopolymer by physical cross-linking with GA has not been investigated. According to our preliminary studies, a thermoreversible gel could be obtained by a physical cross-linking of an unmodified TSX with GA.

An understanding of the sol–gel transition and the physical properties of a gel is essential for the development of a desirable thermoreversible gel. Various techniques have been employed to characterize sol–gel transitions. These include differential scanning calorimetry (DSC),[18] cloud point,[19] light scattering,[20] small angle X-ray scattering (SAXS)[11] and rheology.[21] Micro-DSC with a calorimetric sensitivity of ±0.50 μW is a powerful technique used for determining the phase transition behavior.[22] This

[a]*Drug Delivery System Excellence Center and Department of Pharmaceutical Chemistry, Faculty of Pharmaceutical Sciences, Prince of Songkla University, Hat Yai, Songkhla, 90112 Thailand. E-mail: vimon.t@psu.ac.th*
[b]*School of Mechanical and Aerospace Engineering, Nanyang Technological University, 50 Nanyang Avenue, 639798, Singapore*
[c]*Soft Materials Laboratory, Natural Sciences and Science Education, National Institute of Education, Nanyang Technological University, 1-Nanyang Walk, 637616 Singapore*

technique monitors small amounts of heat consumption or release during the phase transition of a thermoreversible gel. Rheological methods can sensitively determine the sol–gel transition process and characterize the rheological behaviors of a gel. Based on the dynamic viscoelastic properties such as the storage modulus G' and the loss modulus G'' as a function of angular frequency, ω, Winter and Chambon proposed that the gelation point is the point at which $G'(\omega) \approx G''(\omega) \approx \omega^n$.[23–25] Although this method was first described for a chemical gel, it can also be applied to several physical gel systems.[26–28] This power law or scaling law is generalized as:

$$G'(\omega) \approx G''(\omega) \approx \omega^n \; 0 < n < 1 \quad (1)$$

where n is the critical exponent. Accordingly, the loss tangent ($\tan \delta$) becomes independent of angular frequency at the gel point:

$$G''(\omega)/G'(\omega) = \tan \delta = \tan(n\pi/2) \quad (2)$$

Thus the gel point is simply determined from a multi-frequency plot of $\tan \delta$ *vs.* gelation time, temperature, or concentration, depending on which parameter governs the gelation process.[21,29,30]

In this study, novel thermoreversible gels consisting of GA and unmodified TSX were prepared and investigated. Their viscoelastic and thermal properties were determined by rheological and micro-DSC techniques, respectively. The chemical interactions between GA and TSX were investigated using the ^{13}C nuclear magnetic resonance (NMR) technique. Furthermore, the effect of the GA concentration on the morphology of the GA–TSX system was investigated using scanning electron microscopy (SEM).

Experimental

Materials

TSX (molecular weight of 202 kDa (Multiangle laser light scattering, MALLS), and sugar composition of xylose : glucose : galactose : arabinose = 36 : 45 : 16 : 3) was obtained from Megazyme International Ireland Ltd., Wicklow, Ireland. GA was purchased from Fluka Chemie GmbH, Buchs, Switzerland. A stock solution of TSX was prepared by dispersing a required amount of TSX in hot deionized water by a slow homogenizing process using a mechanical stirrer at 50 °C for 4 h. Solutions of GA were prepared by dissolving the required amounts of GA in deionized water at 40 °C. Appropriate volumes of GA solutions were added into the TSX solution and vigorously stirred at 50 °C to obtain 0.2%, 0.4%, 0.6%, 0.8% and 1.0% (w/v) of GA in 1.0% (w/v) TSX.

Rheological measurements

The rheological properties were measured using a strain-controlled rheometer (ARES 100FRTN1, Rheometric Scientific, NJ, USA). The rheometer was equipped with two sensitive force transducers for the torque measurements that ranged from 3.92×10^{-7} to 9.80×10^{-3} N m. Parallel plate geometries with diameters of 25 or 50 mm were used for the relatively high and low viscosity sample solutions, respectively. The high viscosity samples included 0.8 and 1% (w/v) GA in 1% (w/v) TSX, while the low viscosity samples were 0.2%, 0.4% and 0.6% (w/v) GA in 1% (w/v) TSX. Samples in the liquid state were loaded onto the bottom plate of the rheometer at 50 °C and then the temperature was adjusted as required. The periphery of the samples was always covered by a thin layer of low viscosity silicone oil to prevent dehydration. The temperature sweep measurements were carried out at an angular frequency of 2π rad s^{-1} or 1 Hz and at a heating and cooling rate of 0.5 °C min^{-1}.

The dynamic viscoelasticity was measured as a function of angular frequency at a simulated physiological temperature (37 °C). Prior to each measurement, a reasonable time was taken to allow for each sample to reach the desired temperature. All rheological measurements were performed at a suitable shear amplitude in the range of linear viscoelasticity.

Microthermal analysis

A micro-differential scanning calorimeter (VP-DSC micro-calorimeter, Microcal Inc.) was used to determine the thermal properties of the samples during a thermal cycle of heating-to-cooling. The reference cell was filled with deionized water. A slow heating and cooling rate of 0.5 °C min^{-1}, which was the same rate used in the rheological measurements, was employed to determine the details of the thermally induced phase transition of the samples. Furthermore, it was previously reported that the slow-temperature scanning rate (below 0.6 °C min^{-1}) had no effect on the thermograms.[31] After each cycle of measurements was completed, the sample cell was cleaned by a continuous flow of deionized water for more than 1 h.

NMR analysis

The ^{13}C NMR spectra of 1.0% (w/v) TSX, 0.6% (w/v) GA and 0.6% (w/v) GA in 1% (w/v) TSX in deuterium oxide (D_2O) were recorded at 30 °C and 60 °C using a Bruker 300 UltraShield at 75 MHz. Tetramethylsilane (TMS) was used as a reference.

Microscopic observation

Small amounts of the samples were dropped onto a flat glass surface and allowed to equilibrate at room temperature (25 °C). The samples were then freeze-dried overnight under vacuum in a Martin Christ Alpha 1-2 LD freeze dryer. The freeze-dried samples were mounted on double-sided carbon tape and sputter-coated with gold before SEM investigation. They were observed using the SEM instrument (JEOL, JSM 5600LV) operating at 5 kV.

Results and discussion

Dynamic viscoelastic and thermal behaviors on heating and cooling

The structural changes of thermoreversible gels are dependent on the temperature upon heating and cooling and are reflected by the viscoelastic properties of the gels. Therefore, temperature sweep measurements were performed to evaluate the changes in the viscoelasticity and microstructure for a GA–TSX system

during heating and cooling. In addition, the phase transition in the GA–TSX systems was explored by micro-DSC. The heating and cooling cycles of micro-DSC were performed over the same temperature range and at the same scan rate as used in the rheological tests. The temperature dependence of storage modulus G' and loss modulus G'' and the micro-calorimetric results of aqueous 1.0% (w/v) TSX alone and the mixtures of 1.0% (w/v) TSX with various concentrations of GA are shown in Fig. 1 and 2, respectively.

As shown in Fig. 1a, the G' and G'' of TSX alone gradually decreased with increasing temperature. G' is below G'' over the entire range of temperature, indicating that the TSX aqueous solution displayed a typical viscoelastic behavior of a polymer solution. This is in a good agreement with the previous report that native TSX does not produce a gel at either a low or high temperature.[9] For the mixture containing 0.2% (w/v) GA (Fig. 1b), G' was always lower than G''. This demonstrated that this mixture was in a solution state in this temperature range. As shown in Fig. 2, no DSC peaks are observed for 1.0% (w/v) TSX alone and 1.0% (w/v) TSX containing 0.2% (w/v) GA. This thermal behavior supports the rheological behavior that a phase transition did not occur in these solutions on heating and cooling.

The G' and G'' as a function of temperature for the mixtures of 1.0% (w/v) TSX and 0.4, 0.6, 0.8 and 1.0% (w/v) GA are shown in Fig. 1c–f. The G' values of these mixtures were higher than 100 Pa at low temperatures of around 10 °C. These mixtures displayed a gel-like viscoelastic behavior ($G' > G''$) at low temperatures while they exhibited a solution behavior ($G' < G''$) at high temperatures. Thus, gelation of the GA–TSX systems was favored at low temperatures. According to the categories of polysaccharide based sol–gel transitions,[32] these GA–TSX mixtures can be categorized as a cold-set gel that transforms from solution to gel upon cooling. Upon heating, both G' and G'' gradually decreased with increasing temperature. In this region of the lower temperatures, G' values were higher than G'', indicating a viscoelastic behavior of gels. Then, G' decreased sharply with increasing temperature. Although G' decreased at a faster rate than G'', G' was always higher than G''. Afterwards, G' and G'' crossed over each other and the crossover temperature shifted to the right (higher temperature) with increasing GA concentration in the mixtures. The crossover temperatures were

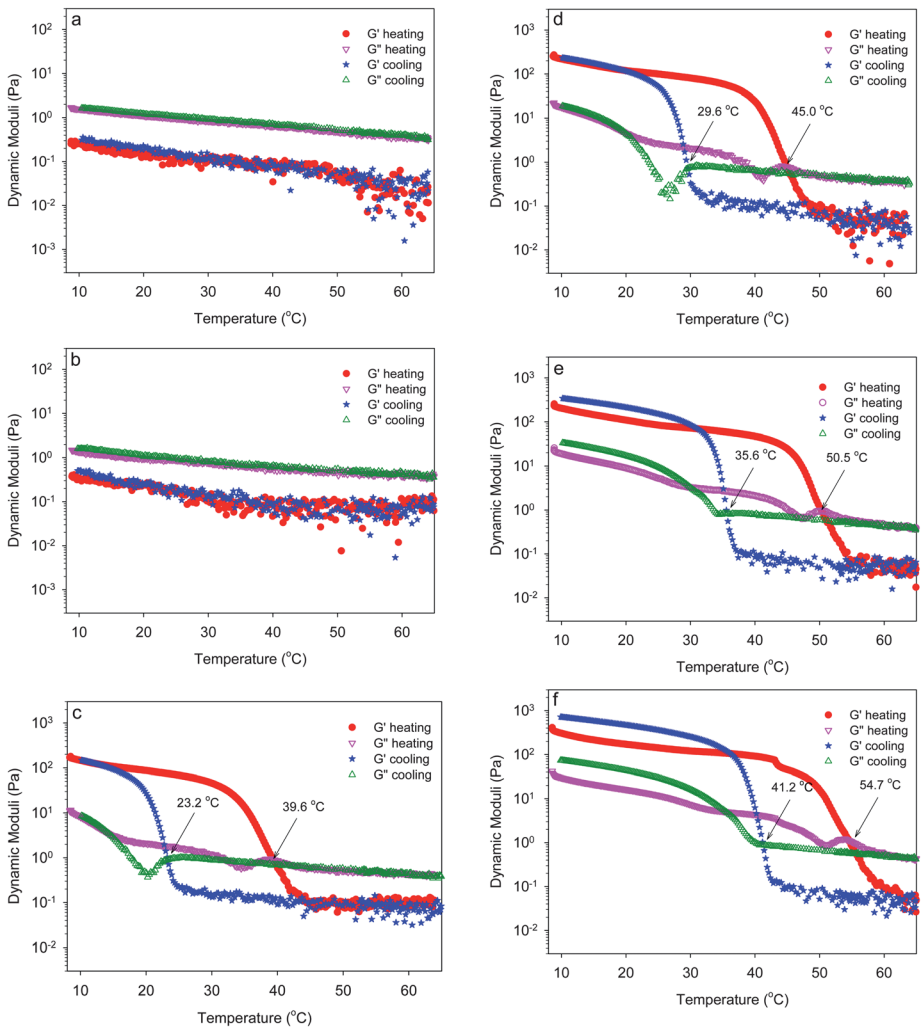

Fig. 1 Temperature dependence of dynamic moduli, G' and G'', for 1.0% (w/v) TSX aqueous solutions containing different concentrations (% w/v) of GA: (a) 0.0 (b) 0.2, (c) 0.4, (d) 0.6, (e) 0.8 and (f) 1.0. The heating and cooling rates were 0.5 °C min^{-1}.

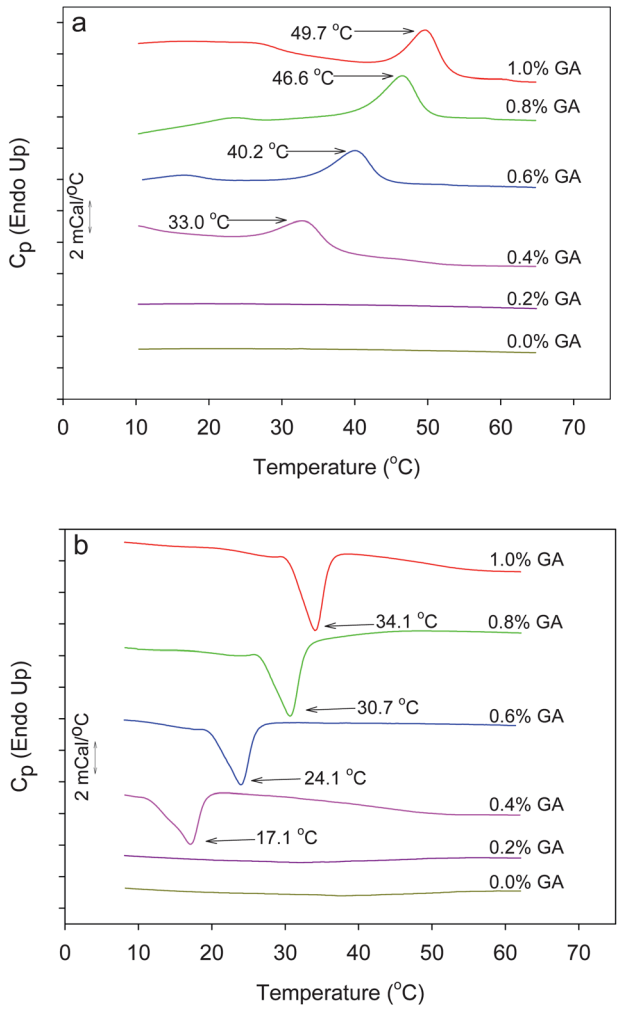

Fig. 2 Calorimetric thermograms of 1.0% (w/v) TSX aqueous solution containing different concentrations of GA upon (a) heating and (b) cooling, at 0.5 °C min^{-1}.

observed at 39.6, 45.0, 50.5 and 54.7 °C for the mixtures containing 0.4, 0.6, 0.8 and 1.0% (w/v) GA, respectively. After this transition temperature, G'' became higher than G' and then gently decreased while G' still declined at a fast rate. Afterwards, both curves seem to reach their own plateaus and remained in parallel with each other.

In the subsequent cooling process, both moduli increased with decreasing temperature. For the mixtures containing 0.4, 0.6, 0.8 and 1% (w/v) GA, G' showed an abrupt increase at 24.8, 30.7, 37.2 and 42.6 °C, respectively. The crossover of G' and G'', which is the indication of a transition from a viscous liquid-like behavior to an elastic gel-like behavior, was observed at 23.2, 29.6, 35.6 and 41.2 °C for the mixtures containing 0.4, 0.6, 0.8 and 1% (w/v) GA, respectively.

According to the micro-DSC analyses, broad endothermic (Fig. 2a) and relatively sharp exothermic peaks (Fig. 2b) were observed for these mixtures upon heating and cooling, respectively. The endothermic peak may be described as the gel-to-sol transition temperature whereas the exothermic peak is the sol-to-gel transition temperature. In addition, the temperatures of the endothermic peaks in the heating DSC curves were higher than those of the exothermic peaks in the cooling DSC curves. The endothermic and exothermic peaks of the mixtures shifted to the higher temperature with increasing GA concentration. As shown in Fig. 2a, the endothermic peaks for the mixtures of 1.0% (w/v) TSX with 0.4, 0.6, 0.8 and 1% (w/v) GA appeared at 33.0, 40.2, 46.6 and 49.7 °C, respectively. Upon cooling, the exothermic peaks were observed at 17.1, 24.1, 30.7 and 34.1 °C for the mixtures containing 0.4, 0.6, 0.8 and 1% (w/v) GA, respectively (Fig. 2b).

To demonstrate the correlation of the rheological properties with the thermal properties of these GA–TSX mixtures upon heating and cooling, the mixture of 1% (w/v) TSX and 0.6% (w/v) GA was used as an example. In the heating process, there were three regions for this mixture. The first region was in the temperature range from 8 °C to about 30 °C. In this region, G' was higher than G'', and both G' and G'' decreased gradually with increasing temperature (Fig. 1d). This indicated that the thermal treatment may weaken the gel network but a three-dimensional gel network may still remain. Accordingly, the DSC heating curve did not show any significant thermal transition peaks in this region (Fig. 2a). The second region started at about 30 °C and ended at about 48 °C beyond which G' reached a plateau (Fig. 1d). In this region, G' decreased steeply with increasing temperature, and then G' became smaller than G''. G' crossed over G'' at 45.0 °C, while the DSC heating curve showed an endothermic peak at 40.2 °C (Fig. 2a). It is noted that the endothermic peak ended at about 45.2 °C, which is close to the cross-over temperature of 45.0 °C. Therefore, we may consider that the disassociation of the gel network proceeds with supplying the endothermic heat. As long as the gel network was destroyed, further endothermic heat was not needed. The third region was after the steep decrease in G', when G' reached its plateau, and where G'' predominated over G' (Fig. 1d). This is indicative of a typical viscoelastic behavior of a polymer solution.

In the subsequent cooling process, three important regions were defined. The first region ranged from the highest temperature to about 32 °C. In this region, both G' and G'' slowly increased with decreasing temperature (Fig. 1d) and no thermal transitions were observed from the DSC curve (Fig. 2b). The second region began at 32 °C, from which G' started to increase sharply, and ended at about 19 °C, at which point the gel returns to its original modulus (Fig. 1d). The crossover temperature of G' and G'' appeared at 29.6 °C while an exothermic peak was shown at 24.1 °C (Fig. 2b). The offset temperature (about 19.3 °C) of the exothermic peak was consistent with the end temperature of the second region, indicating that the gelation was completed during the second region. The third region followed the second region after the sol–gel transition and the complete formation of the gel network. In this region, both moduli still gradually increased with decreasing temperature mainly due to the effect of thermal contraction rather than the formation of new joints upon cooling (Fig. 1d).

As shown in Fig. 1e and f, both G' and G'' on cooling were larger than those on heating. This occurred only for the mixtures with higher concentration of GA, namely 0.8 and 1% (w/v). One explanation for this phenomenon is that the systems may not be thermally reversible.[33] However, this explanation is not consistent with the GA–TSX systems since the GA–TSX systems are

thermoreversible (see discussion below). Thus the increase of both G' and G'' upon cooling could be due to the fact that with the higher concentration of GA, the gelation process after the transition temperature is more effective from the rheological point of view, as previously described by Wietor *et al.*[34]

Furthermore, the dependence of the gelation and degelation temperatures on the GA concentration in the 1% (w/v) TSX aqueous solution was examined and the results are shown in Fig. 3. The transition temperatures characterized by micro-DSC and rheological measurements were the endothermic or exothermic peak temperatures and the crossover temperatures of the dynamic moduli G' and G'', respectively. The gelation and gel melting temperatures obtained by rheological and micro-DSC measurements were increased linearly with increasing GA concentration. Based on the micro-DSC measurement, the endothermic peak is considered as the breakup of hydrogen bonds whereas the exothermic peak is regarded as the formation of hydrogen bonds of the gelling systems.[35–37] In addition, the dissociation of hydrogen bonds, which is endothermic in some gelling systems, can occur at low temperatures such as 22 to 40 °C.[37] Furthermore, the formation and dissociation of hydrogen bonds upon cooling and heating in the gels can be related to the network structures as previously studied.[37] In this study, the increase of GA molecules in the system can increase the number of hydrogen bonds formed between GA molecules and TSX chains, which is corresponding to an increase in the number of junctions of gel networks and/or the stabilization of junctions in the gels. Therefore, the higher gel melting temperature is needed to break up the gel system containing more GA molecules. The increase of the gelation temperatures in the cooling process can be described by a similar mechanism.

It should be noted that the gelation and gel melting temperature values obtained by the rheological measurements and micro-DSC measurements were not exactly the same. The small differences between these values could be attributed to the variations in sensitivity and the measurement principle of each method.[19,38] The micro-DSC detects the amount of heat absorbed or released, *i.e.* energy changes, by a sample during a thermally induced gel–sol or sol–gel transition, respectively. The rheological measurement reveals the change in viscoelasticity for a sample. In the heating process, heat absorption occurred first to cause the destruction of the hydrogen bonds in the junction zones of a GA–TSX gel. In the next step, the deaggregation of the chain clusters resulted in the viscous character so that a crossover point was observed in the viscoelastic spectra. Therefore, in the heating process, the gel melting temperatures obtained by the rheological measurement appeared later (or are higher) than the gel melting temperatures obtained by the micro-DSC. In the cooling process, the aggregation and connection of the dispersed TSX chains through hydrogen bonding with GA resulted in an increase of the elastic components. As a result, the elastic character predominated and a gel was then formed. The reason for the gelation temperatures obtained by the micro-DSC being always lower than those obtained by the rheological measurement was because of (i) the difference in sensitivity and (ii) the difference in the definition of a gelation or gel melting temperature between the two methods. First, thermal sensitivity to the sol–gel transition relies on the gelation mechanism. If the formation of a gel network is simultaneously accompanied by heat absorption or heat release, a thermal method like micro-DSC works as well as a rheological method for determination of a gel point. If heat absorption or heat release is a precursor of gelation in a cooling process, however, the thermally determined gel point will be higher than the rheologically determined one. In contrast, the thermally determined gel point will be lower than the rheologically determined one. Second, the difference in the definition of gelation and degelation temperatures between the two methods may result in a difference in the value of these temperatures. In Fig. 3, the gel melting and gelation temperatures determined by micro-DSC are defined by the endothermic and exothermic peak temperatures, respectively, while the temperatures acquired by rheology are defined by the crossover temperatures of G' and G''. Since a gelling system would not necessarily exhibit the maximum heat absorption or heat release at the crossover temperature of G' and G'', the differences in the gelation and degelation temperatures between two methods would appear. No other theoretical arguments have been found in the literature for the consistencies or contradictions between a thermally determined gel point and a rheologically determined one. An additional and important point we should note here is that the crossover temperatures of G' and G'' are frequency-dependent.

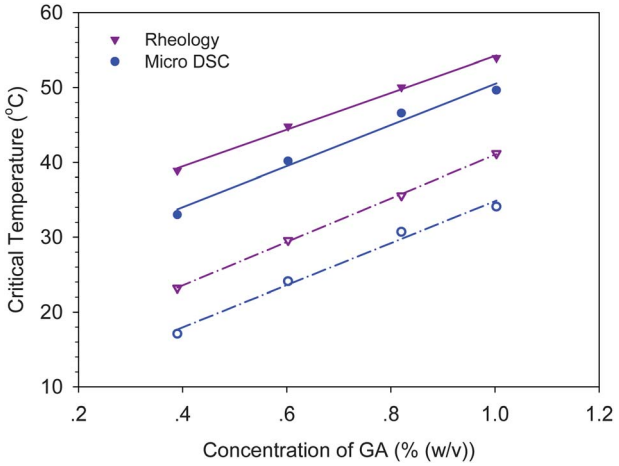

Fig. 3 Critical temperatures of 1.0% (w/v) TSX aqueous solution containing different concentrations of GA for two methods upon heating (closed symbol) and cooling (opened symbol).

Heat absorption (*i.e.* integrated area under the endothermic peak) during a gel–sol transition is considered to be the total energy required to destroy the entire gel network. In other words, it reflects the interaction between TSX and GA: the greater the interaction, the larger the heat absorption. The relationship between the heat absorption and the concentration of GA in the mixtures of 1% (w/v) TSX is shown in Fig. 4. The values for heat absorption increased linearly with increasing GA concentration. Such a linear effect of the GA concentration on the heat absorption could result from the linear increase of hydrogen bonds formed between TSX and added GA with increasing GA concentration. Thus the formation of a thermally stable TSX gel was favored when the GA concentration was increased.

According to both rheological and micro-DSC analyses, the temperature sweep curves for gelling mixtures in the heating and

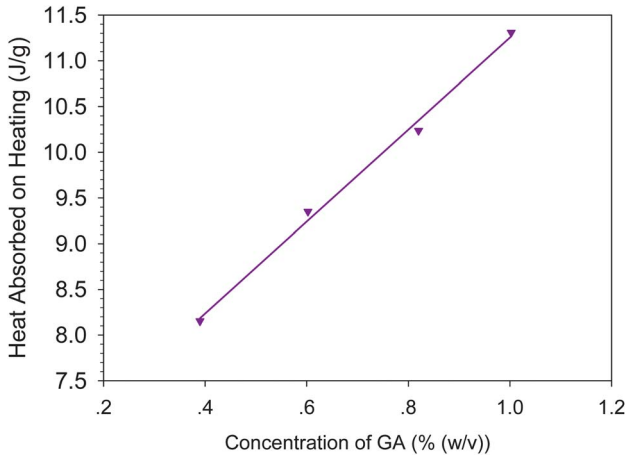

Fig. 4 Heat absorbed on heating as a function of GA concentration in 1.0% (w/v) TSX.

cooling processes indicated that the phase transitions were thermoreversible. The thermoreversibility of a gel is simply verified by running two thermal cycles from heating to cooling at the same scan rate and then comparing the calorimetric thermograms for the two cycles.[39,40] The two heating thermograms and the two cooling thermograms for 1% (w/v) TSX containing 1% (w/v) GA, which were obtained through two consecutive thermal cycles at a scan rate of 0.5 °C min^{-1}, are shown in Fig. 5. The data are shifted along their vertical axes by arbitrary amounts to avoid overlapping. For the heating and cooling processes, the first-cycle curves and the second-cycle curves overlapped perfectly if the second-cycle curves were superimposed on the first-cycle curves. The overlaps between the two different cycles in the heating and cooling processes were also observed at other GA concentrations. The results indicated that the GA–TSX gels were perfectly thermoreversible. The mixtures of 1.0% (w/v) TSX and 0.4, 0.6, 0.8 and 1.0% (w/v) GA exhibited thermal hysteresis during a thermal cycle from heating to cooling since the gelling temperature was significantly lower than the melting temperature as observed by both the micro-DSC and the

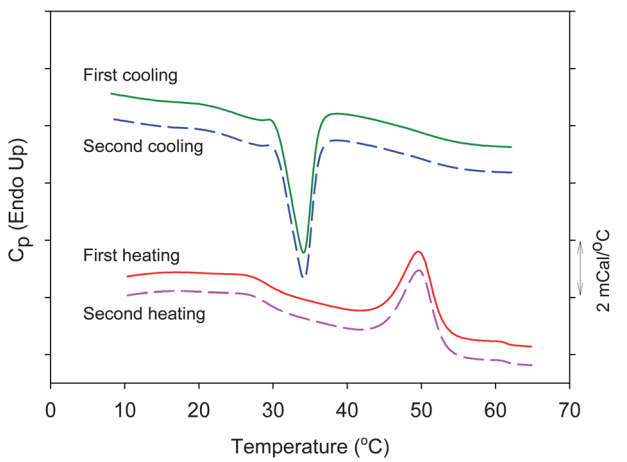

Fig. 5 Calorimetric thermograms of 1.0% (w/v) GA in 1.0% (w/v) TSX during two thermal cycles at the same heating and cooling rates of 0.5 °C min^{-1}.

rheological measurements. Thermal hysteresis was detected for various gelling systems such as the gellan–TSX system,[41] alginate in the presence of potassium salt[42] and agarose gel.[43] As described by Djabourov and Papon,[44] the origin of the hysteresis is not completely understood. However, there are various explanations for hysteresis. For a thermoreversible physical gel, the thermal hysteresis is usually caused by the stabilization of the system by further aggregation of polymer chains.[45,46] These stabilized aggregates remain stable at higher temperature than those that are formed on cooling. For helix forming polysaccharide, the energy for breaking up the helix aggregate is suggested to be higher than the energy for gel formation.[47] The very strong aggregation of these polymer chains can stabilize the helices during a temperature ramp which will result in different transition temperatures between heating and cooling.[48] In addition, the stability of the double helix aggregation can be altered by modifications such as adding co-solutes, using a mixture of solvents or changing pH.[48,49] Other polysaccharides, such as alginate, do not exhibit a coil–helix transformation during gelation. The intermolecular interaction between these polymer chains and the salt ions leads to the formation of junction zones.[42] Furthermore, the additional hydrogen bonds may also cause hysteresis in some gel systems.[50] Hydrogen bonds could function as cross-linking points between different chains, as previously described,[50] in a similar manner to the cross-linking of alginate by salt. Native TSX chains in aqueous solution do not have the coil–helix transforming property. The presence of thermal hysteresis of GA–TSX could suggest the existence of a stabilized network and this is possibly caused by intermolecular hydrogen bonding that acts as a cross-link between TSX chains by GA molecules.

NMR analysis

TSX has a cellulose backbone of (1 → 4)-β-D-glucose, and about 80% of this chain is substituted with (1 → 6)-α-xylose. In addition, some xylose residues are further substituted with (1 → 2)-β-galactose.[9] Based on the molecular structures of GA, as shown in Fig. 6, GA and TSX both contain hydrogen bond donors and acceptors. Therefore, the gelation of a GA–TSX mixture is expected to be caused by the formation of hydrogen bonds between the OH groups of the TSX chains and the GA molecules. The presence of a chemical interaction between GA and TSX was investigated with ^{13}C NMR using the mixture of 0.6% GA–TSX as well as the corresponding concentrations of GA and TSX alone for comparison. The mixture of 0.6% GA–TSX becomes a gel at a low temperature such as 30 °C and a sol at a high temperature *i.e.* 60 °C. All samples were then measured at 30 and 60 °C and their ^{13}C NMR spectra are shown in Fig. 6. The chemical shifts (δ) for the carboxyl carbon (C7), C3 and C5, C4, C1, and C2, and C6 of GA (Fig. 6) at 30 and 60 °C are listed in Table 1. C3 and C5 have the same δ values since both are equivalent. The δ values for C2 and C6 are also similar due to the equivalence of both atoms. These δ values for GA are comparable to those previously reported.[51] The ^{13}C NMR spectra of TSX showed signals for C1 of each sugar unit in the region of about 95–105 ppm and other signals at the region of 60–80 ppm, as shown in Fig. 6. The δ values for the C1 of galactose, glucose and xylose, respectively, are observed at 104.04, 102.45 and

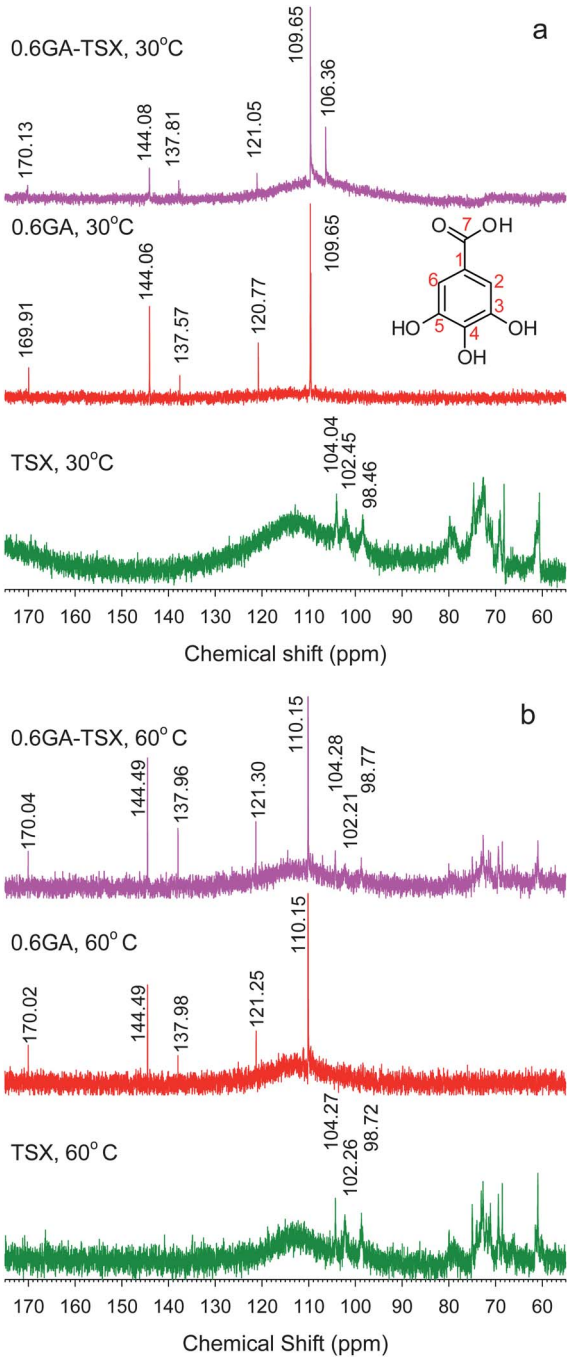

Fig. 6 ^{13}C NMR spectra of 0.6% (w/v) GA alone and 0.6% (w/v) GA-1% (w/v) TSX at 30 and 60 °C.

Table 1 ^{13}C NMR chemical shifts of 0.6% (w/v) GA alone and GA in the 0.6% (w/v) GA-1% (w/v) TSX mixture at 30 and 60 °C

		Chemical shift (ppm)				
		C7	C3, C5	C4	C1	C2, C6
30 °C	GA	169.91	144.06	137.57	120.77	109.65
	GA–TSX	170.13	144.08	137.81	121.05	109.65
60 °C	GA	170.02	144.49	137.98	121.25	110.15
	GA–TSX	170.04	144.49	137.96	121.30	110.15

98.46 ppm (Fig. 6a) when the sample was measured at 30 °C, and at 104.27, 102.26, and 98.72 ppm (Fig. 6b) when the spectrum was obtained at 60 °C. These chemical shifts are comparable to the reported values.[52]

The δ values for all GA carbon atoms of 0.6% GA–TSX at 30 and 60 °C are also shown in Table 1. At 30 °C, a downfield shift ($\Delta\delta$) of 0.22, 0.24 and 0.28, respectively, for the C7, C4, and C1, compared to the corresponding signals for the 0.6% GA alone, was detected. This reflects the decrease of electron density of these carbon atoms of GA in the GA–TSX gel. The downfield shifts of C7 and C4 could be caused by hydrogen bond interactions of COOH and OH at position 4 of the GA with TSX. However, the reduction of electron density at C1 might be caused by the resonance and inductive effects from the OH at C4 and the COOH attached to the C1, respectively.

As shown in Fig. 6a, a signal at 106.36 ppm was the only one observed for TSX in the GA–TSX gel while the other signals disappeared. The loss of the ^{13}C NMR signals in some gel systems has been previously reported.[53,54] The loss of NMR signals has been previously described due to the immobilization of the polymer chain as a result of the presence of physical cross-links *via* intermolecular hydrogen bonds.[53,54] For the GA–TSX gel system, the hydrogen bonds between TSX and both the COOH and OH at C4 of GA could immobilize the TSX chain resulting in the loss of signals of TSX.

At 60 °C, the 0.6% GA–TSX was in the sol state. The ^{13}C NMR spectrum of TSX in GA–TSX at 60 °C is shown in Fig. 6b. In contrast to the GA–TSX gel, all characteristic peaks of TSX were observed in this GA–TSX sol. Most of the GA signals remain at the same δ values. This might suggest that GA did not interact with TSX at this temperature. Consequently, the mixture remained in the sol state.

Dynamic viscoelastic behavior at physiological temperature

The viscoelasticity of a gel at a physiological temperature is important for its possible application as a biomaterial because most of the biomaterials are used under physiological conditions. Therefore, the frequency sweep measurements were performed to investigate the viscoelastic behavior of the GA–TSX system at 37 °C. The angular frequency dependence of the dynamic moduli for all samples is shown in Fig. 7. The viscoelastic behaviors of the samples were dependent on the GA concentration. Both dynamic moduli of a 1.0% (w/v) TSX solution and 1% (w/v) TSX solutions containing 0.2%, 0.4% and 0.6% (w/v) GA are frequency-dependent and increase with frequency. G'' is higher than G' in the entire frequency range and the difference between G'' and G' became smaller at high angular frequencies. This pattern clearly demonstrated that the samples possess a common viscoelastic behavior of a concentrated polymer solution. In general, G' values at low angular frequencies are too small to be measured accurately due to the experimental detection limit of a rheometer,[55] so fluctuations of G' are observed at low angular frequencies.

For a polymer solution, G' and G'' generally exhibit a low frequency terminal behavior: $G'(\omega) \approx \omega^2$ and $G''(\omega) \sim \omega^1$ (at $\omega \rightarrow 0$), which is consistent with the viscoelastic liquid.[56] The slopes of $G'(\omega)$ *versus* ω curves for 1.0% (w/v) TSX and its mixture containing 0.2% (w/v) GA were 1.5 and 1.3, respectively.

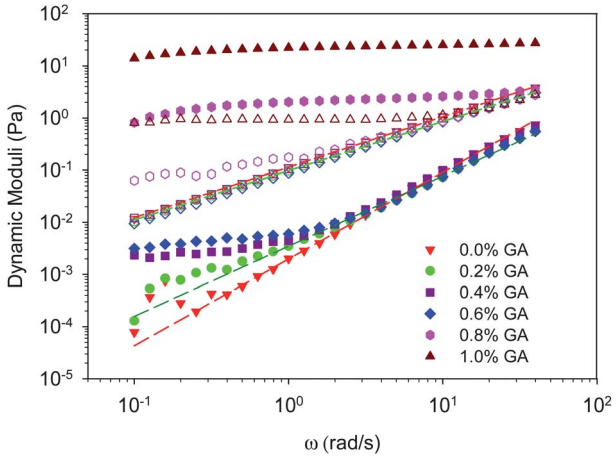

Fig. 7 Angular frequency ω dependence of storage (G', closed) and loss (G'', opened) moduli for 1.0% (w/v) TSX aqueous solution containing various concentrations of GA at 37 °C.

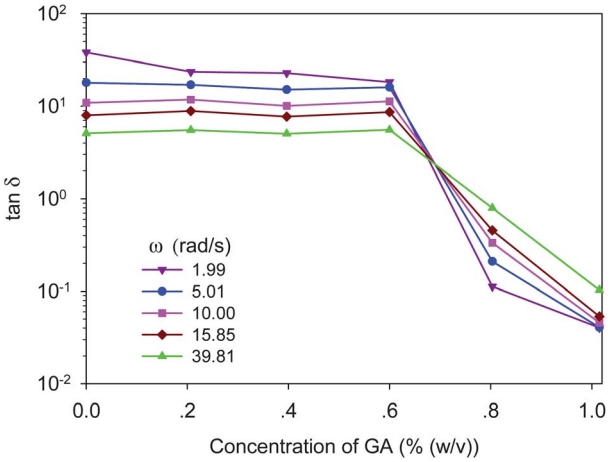

Fig. 8 Tan δ at indicated ω plotted against GA concentration for 1.0% (w/v) TSX aqueous solutions containing various concentrations of GA at 37 °C.

The slopes of G'' *versus* ω curves for both solutions were 0.9. The deviations from the expected slopes probably resulted from the polydispersity of TSX as previously observed for methylcellulose,[57] λ-carrageenan[58] and guar solutions[59] or from the relatively high concentration of TSX in the solutions. The deviation became more significant for the mixtures containing 0.4 and 0.6% (w/v) GA. The G' curves of both mixtures showed a plateau-like behavior in the low frequency range. The G' plateaus are believed to be due to weak reversible association of polymer chains[29,57,60] as well as to weak hydrogen bonding between TSX chains and GA molecules. Such physical association of TSX chains in these viscoelastic fluids was strengthened by increasing the GA concentration.

For 0.8% (w/v) GA in 1.0% (w/v) TSX, G' became higher and flatter than G'' while G'' increased with frequency. This behavior indicated the formation of a three-dimensional gel network.[61] In the GA–TSX mixtures, TSX chains could associate through GA–TSX interactions to form aggregates. Afterward, the aggregation of TSX chains led to the formation of a three-dimensional network. For the mixture containing 1.0% (w/v) GA, G' values were relatively constant over the entire angular frequency range and were ten times higher than their G'' values. A gel with this behavior can be defined as a strong gel.[62,63]

The sol–gel transition and scaling law at physiological temperature

Determination of the critical gel concentration (C_g) of GA at the sol–gel transition point is important for us to understand how the concentration of GA governs the gelation of TSX and how GA affects the macroscopic properties of a TSX gel. In this study, a theoretical approach was applied to determine the critical gel concentration (C_g) of GA at 37 °C.

The frequency independence of tan δ at the sol–gel transition according to the Winter–Chambon criterion (eqn (1) and (2)) was used to determine the critical gel point for the mixtures of GA–TSX. This method has been accurately verified for various physically gelling systems.[21,55] Using this method, the C_g, the minimum GA concentration required for the gelation of an aqueous mixture of GA and 1% (w/v) TSX, was determined from the multifrequency plots of tan δ *versus* GA concentration. As shown in Fig. 8, tan δ values at various frequencies decreased with increasing GA concentration. This indicated that the mixtures with a higher GA concentration were more elastic. All tan δ curves intersected each other at a common point of approximately 0.69% (w/v) GA. This indicated that a gel was able to form from a mixture of GA–TSX when the GA concentration was equal to or higher than 0.69% (w/v). Therefore, the sol–gel transition behavior of the GA–TSX system was well described by the scaling law.

The scaling exponent n is generally recognized as a valuable descriptor that reflects the local structure of polymeric gels.[55] This exponent is computed from the gel point using eqn (2). According to Winter and Mours,[64] a stiffer critical gel generally has a small value of n ($0 < n < 0.5$) while the n value for a soft and fragile critical gel is large ($0.5 < n < 1$). Although the theoretical predictive value of n is between 2/3 and 1,[65,66] experimental values of n are often between 0 and 1.[21,24,25,55,67–69] Thus there is no general value for n since this value depends on the specific nature of each gelling system. The n value for the GA–TSX mixture at 37 °C calculated using eqn (2) was 0.75. Therefore, the GA–TSX critical gel was most likely to be a soft gel.

Morphological properties

The morphology of freeze-dried TSX and the mixtures of GA–TSX was determined by SEM. As shown in Fig. 9a and b, porous morphologies are observed for TSX alone and the mixture of 0.2% GA–TSX. These porous morphologies have previously been observed for the modified TSX.[70] The freeze-dried gels from the mixtures of 1% (w/v) TSX and higher concentrations (0.4, 0.6% w/v) of GA showed both porous and fibrillar morphologies (Fig. 9c and d). As shown in Fig. 9e, more fibrillar morphologies were observed for the higher GA concentration of 0.8% (w/v). It is of interest that a homogeneously fibrillar morphology was obtained from the gel with 1% GA–TSX (Fig. 9f). Since GA can

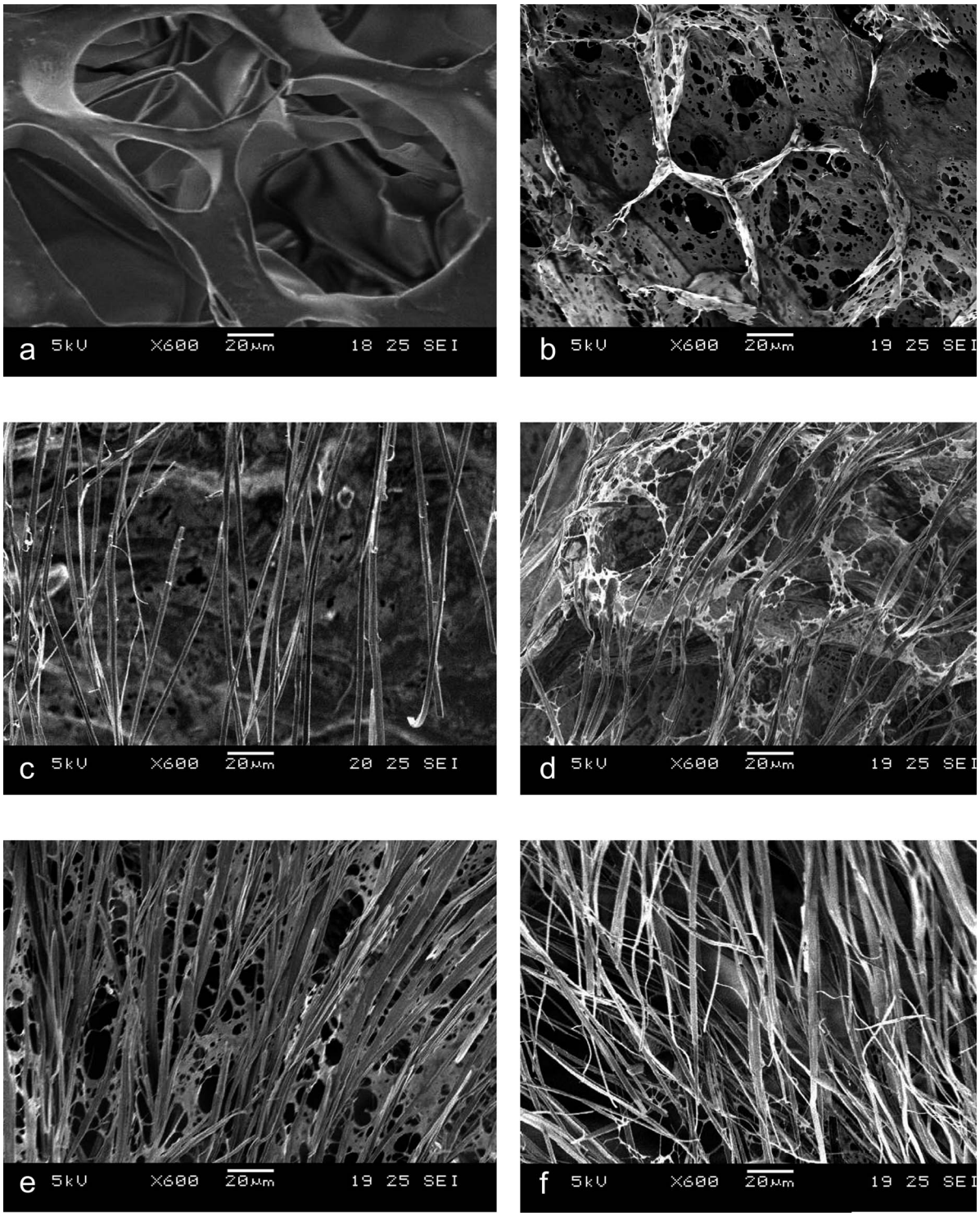

Fig. 9 SEM images of freeze-dried 1.0% (w/v) TSX aqueous solutions containing different concentrations of GA (% w/v): (a) 0.0, (b) 0.2, (c) 0.4, (d) 0.6, (e) 0.8 and (f) 1.0.

form hydrogen bonds with TSX, these interactions between GA and TSX could affect the structures or the gel networks to reflect their fibrillar morphologies. Furthermore, a higher concentration of GA could interact more with the TSX and promote more TSX chains to associate into a more fibrillar morphology as shown in Fig. 9c–f.

Conclusions

The aqueous solution of TSX (1% w/v) was unable to form a gel but GA was able to induce the gelation of TSX. The GA–TSX gels are completely thermoreversible. According to the rheological studies, these GA–TSX gels could be classified as a cold-set

gel. In addition, the hydrogen bonds between GA and TSX were revealed using NMR analyses. The gel networks are formed by hydrogen bonding at GA–TSX junction zones. The hysteresis in a heating to cooling cycle is observed for these GA–TSX gelling systems. Furthermore, the gelation and degelation temperatures shifted to a higher temperature with increasing GA concentration. Moreover, a linear GA concentration dependence of the heat absorption was observed. The ^{13}C NMR analyses indicated that the OH at C4 and the COOH group of GA interacted with TSX in the GA–TSX gel based on the significant downfield shifts of C4, C1 and C7 of GA as well as the loss of signals from TSX. In addition, no significant interaction between GA and TSX was revealed for the GA–TSX mixture at the sol state.

The viscoelastic behavior at physiological temperature depended on the concentration of GA. A strong viscoelastic gel was formed in the GA–TSX mixture containing 1% (w/v) GA. The critical gel concentration was well described by the scaling law. Moreover, it was verified by SEM that the fibrillar structures of the GA–TSX gel were present at relatively high concentrations of GA due to the strong intermolecular hydrogen bonding between GA and TSX, as confirmed by the ^{13}C NMR analyses.

The results obtained from micro-DSC, rheology, NMR and SEM have provided valuable information on the GA–TSX thermoreversible gels. The adjustable properties of GA–TSX gels simply by changing the concentration of GA would most likely allow them to be developed into biomaterials for biomedical applications in the near future.

Acknowledgements

This work was supported by the Higher Education Research Promotion and National Research University Project of Thailand, Office of the Higher Education Commission and the Thailand Research Fund through the Royal Golden Jubilee Ph.D. Program through grant no. PHD/0259/2549. The authors would like to thank Ms Yupparase Pullaput for measuring the ^{13}C NMR spectra.

References

1 A. Saxena, M. Kaloti and H. B. Bohidar, *Int. J. Biol. Macromol.*, 2011, **48**, 263.
2 T. R. Hoare and D. S. Kohane, *Polymer*, 2008, **49**, 1993.
3 F. Ilmain, T. Tanaka and E. Kokufuta, *Nature*, 1991, **349**, 400.
4 S. V. Vlierberghe, E. Schacht and P. Dubruel, *Eur. Polym. J.*, 2011, **47**, 1039.
5 H. Urakawa, M. Mimura and K. Kajiwara, *Trends Glycosci. Glycotechnol.*, 2002, **14**, 355.
6 M. Sano, E. Miyata, S. Tamano, A. Hagiwara, N. Ito and T. Shirai, *Food Chem. Toxicol.*, 1996, **34**, 463.
7 E. Ghelardi, A. Tavanti, P. Davini, F. Celandroni, S. Salvetti, E. Parisio, E. Boldrini, S. Senesi and M. Campa, *Antimicrob. Agents Chemother.*, 2004, **48**, 3396.
8 F. Suisha, N. Kawasaki, S. Miyazaki, M. Shirakawa, K. Yamatoya, M. Sasaki and D. Attwood, *Int. J. Pharm.*, 1998, **172**, 27.
9 M. Shirakawa, K. Yamatoya and K. Nishinari, *Food Hydrocolloid*, 1998, **12**, 25.
10 N. Hirun, V. Tantishaiyakul and W. Pichayakorn, *Int. J. Pharm.*, 2010, **388**, 196.
11 Y. Yuguchi, T. Kumagai, M. Wu, T. Hirotsu and J. Hosokawa, *Cellulose*, 2004, **11**, 203.
12 Y. Yuguchi, T. Fujiwara, H. Miwa, M. Shirakawa and H. Yajima, *Macromol. Rapid Commun.*, 2005, **26**, 1315.
13 Y. Yuguchi, T. Hirotsu and J. Hosokawa, *Cellulose*, 2005, **12**, 469.
14 M. Inoue, R. Suzuki, T. Koide, N. Sakaguchi, Y. Ogihara and Y. Yabu, *Biochem. Biophys. Res. Commun.*, 1994, **204**, 898.
15 B.-C. Ji, W.-H. Hsu, J.-S. Yang, T.-C. Hsia, C.-C. Lu, J.-H. Chiang, J.-L. Yang, C.-H. Lin, J.-J. Lin, L.-J. W. Suen, W. G. Wood and J.-G. Chung, *J. Agric. Food Chem.*, 2009, **57**, 7596.
16 D. H. Priscilla and P. S. M. Prince, *Chem.-Biol. Interact.*, 2009, **179**, 118.
17 A. Saha, B. Roy, A. Garai and A. K. Nandi, *Langmuir*, 2009, **25**, 8457.
18 Y. Xu, L. Li, P. Zheng, Y. C. Lam and X. Hu, *Langmuir*, 2004, **20**, 6134.
19 Y. Xu and L. Li, *Polymer*, 2005, **46**, 7410.
20 D. G. Lessard, M. Ousalem, X. X. Zhu, A. Eisenberg and P. J. Carreau, *J. Polym. Sci., Part B: Polym. Phys.*, 2003, **41**, 1627.
21 L. Li and Y. Aoki, *Macromolecules*, 1997, **30**, 7835.
22 S. Gaisford, in *Thermal Analysis of Pharmaceutics*, ed. D. Q. M. Craig and M. Reading, CRC Press, New York, 2006.
23 F. Chambon and H. H. Winter, *Polym. Bull.*, 1985, **13**, 499.
24 H. H. Winter and C. Francois, *J. Rheol.*, 1986, **30**, 367.
25 C. Francois and H. H. Winter, *J. Rheol.*, 1987, **31**, 683.
26 T. Fuchs, W. Richtering, W. Burchard, K. Kajiwarab and S. Kitamura, *Polym. Gels Networks*, 1997, **5**, 541.
27 H. W. Richtering, K. D. Gagnon, R. W. Lenz, R. C. Fuller and H. H. Winter, *Macromolecules*, 1992, **25**, 2429.
28 Y. Fang and K. Nishinari, *Biopolymers*, 2004, **73**, 44.
29 L. Li, *Macromolecules*, 2002, **35**, 5990.
30 Y. Nitta, B. S. Kim, K. Nishinari, M. Shirakawa, K. Yamatoya, T. Oomoto and I. Asai, *Biomacromolecules*, 2003, **4**, 1654.
31 C. Hofmann and M. Schönhoff, *Colloid Polym. Sci.*, 2009, **287**, 1369.
32 K. Nishinari, in *Comprehensive Handbook of Calorimetry and Thermal Analysis*, ed. M. Sorai, John Wiley & Sons, West Sussex, 2004.
33 B. Roy, P. Bairi, A. Saha and A. K. Nandi, *Soft Matter*, 2011, **7**, 8067.
34 J.-L. Wietor, D. J. M. van Beek, G. W. Peters, E. Mendes and R. P. Sijbesma, *Macromolecules*, 2011, **44**, 1211.
35 Y. Jin, H. Zhang, Y. Yin and K. Nishinari, *Carbohydr. Res.*, 2006, **341**, 90.
36 H. B. Zhang, K. Nishinari, M. A. K. Williams, T. J. Foster and I. T. Norton, *Int. J. Biol. Macromol.*, 2002, **30**, 7.
37 H. Dai, Q. Chen, H. Qin, Y. Guan, D. Shen, Y. Hua, Y. Tang and J. Xu, *Macromolecules*, 2006, **39**, 6584.
38 M. Tomsic, F. Prossnigg and O. Glatter, *J. Colloid Interface Sci.*, 2008, **322**, 41.
39 L. Li, H. Shan, C. Y. Yue, Y. C. Lam, K. C. Tam and X. Hu, *Langmuir*, 2002, **18**, 7291.
40 M. A. Villetti, C. I. D. Bica, I. T. S. Garcia, F. V. Pereira, F. I. Ziembowicz, C. L. Kloster and C. Giacomelli, *J. Phys. Chem. B*, 2011, **115**, 5868.
41 K. Nishinari, B. Kim, Y. Fang, Y. Nitta and M. Takemasa, *Cellulose*, 2006, **13**, 365.
42 C. Karakasyan, M. Legros, S. Lack, F. Brunel, P. Maingault, G. Ducouret and D. Hourdet, *Biomacromolecules*, 2010, **11**, 2966.
43 Z. H. Mohammed, M. W. N. Hember, R. K. Richardson and E. R. Morris, *Carbohydr. Polym.*, 1998, **36**, 15.
44 M. Djabourov and P. Papon, *Polymer*, 1983, **24**, 537.
45 E. R. Morris, D. A. Rees and G. Robinson, *J. Mol. Biol.*, 1980, **138**, 349.
46 J. N. Liang, E. S. Stevens, E. R. Morris and D. A. Rees, *Biopolymers*, 1979, **18**, 327.
47 J. P. Arnaud, I. Choplin and C. Lacrox, *J. Texture Stud.*, 1988, **19**, 419.
48 M. W. N. Member and E. R. Morris, *Carbohydr. Polym.*, 1995, **27**, 23.
49 C. S. F. Picone and R. L. Cunha, *Carbohydr. Polym.*, 2011, **84**, 662.
50 H. Cheng, L. Shen and C. Wu, *Macromolecules*, 2006, **39**, 2325.
51 R. C. Latha and P. Daisy, *Chem.-Biol. Interact.*, 2011, **189**, 112.
52 M. J. Gidley, P. J. Lillford, D. W. Rowlands, P. Lang, M. Dentini, V. Crescenzi, M. Edwards, C. Fanutti and J. S. Reid, *Carbohydr. Res.*, 1991, **214**, 299.
53 H. Saitô, T. Ohki and T. Sasaki, *Biochemistry*, 1977, **16**, 908.
54 H. Saitô, T. Ohki and T. Sasaki, *Carbohydr. Res.*, 1979, **74**, 227.
55 L. Lu, X. Liu, L. Dai and Z. Tong, *Biomacromolecules*, 2005, **6**, 2150.
56 J. D. Ferry, *Viscoelastic Properties of Polymers*, John Wiley & Sons, USA, 3rd edn, 1980.
57 K. Kobayashi, C.-i. Huang and T. P. Lodge, *Macromolecules*, 1999, **32**, 7070.
58 A. H. Clark and S. B. Ross-Murphy, *Adv. Polym. Sci.*, 1987, **83**, 57.

59 E. R. Morris, in *Gums and Stabilizers for the Food Industry*, ed. G. O. Phillips, D. J. Wedlock and P. A. Williams, Pergamon, Oxford, 1984, vol. 2.
60 K. Chakrabarty, L.-Y. Shao and R. A. Weiss, in *Ionomers: Synthesis, Structure, Properties, and Applications*, ed. M. R. Tant, K. A. Mauritz and G. L. Wilkes, Chapman & Hall, London, 1997.
61 D. Ruan, A. Lue and L. Zhang, *Polymer*, 2008, **49**, 1027.
62 A. Marĺnez-Ruvalcaba, E. Chornet and D. Rodrigue, *Carbohydr. Polym.*, 2007, **67**, 586.
63 B. B. Mandal, S. Kapoor and S. C. Kundu, *Biomaterials*, 2009, **30**, 2826.
64 H. H. Winter and M. Mours, *Adv. Polym. Sci.*, 1997, **134**, 165.
65 J. E. Martin, D. Adolf and J. P. Wilcoxon, *Phys. Rev. Lett.*, 1988, **61**, 2620.
66 J. E. Martin and D. Adolf, *Annu. Rev. Phys. Chem.*, 1991, **42**, 311.
67 K. Te Nijenhuis and H. H. Winter, *Macromolecules*, 1989, **22**, 411.
68 J. C. Scanlan and H. H. Winter, *Macromolecules*, 1991, **24**, 47.
69 R. Hernández, J. Sacristán and C. Mijangos, *Macromol. Chem. Phys.*, 2010, **211**, 1254.
70 D. R. Nisbet, K. E. Crompton, S. D. Hamilton, S. Shirakawa, R. J. Prankerd, D. I. Finkelstein, M. K. Horne and J. S. Forsythe, *Biophys. Chem.*, 2006, **121**, 14.

Addition and correction

Note from RSC Publishing

This article was originally published with incorrect page numbers. This is the corrected, final version.

The Royal Society of Chemistry apologises for these errors and any consequent inconvenience to authors and readers.